

# Ahmed Zaki\*, Yasmeen Elberry, Hamad Al-Ajami, Mostafa Rabah, and Rasha Abd El Ghany

# Determination of local geometric geoid model for Kuwait

<https://doi.org/10.1515/jag-2022-0017>

Received June 1, 2022; accepted July 10, 2022

**Abstract:** Determining a precise local geoid is particularly important for converting the Global Navigation Satellite System (GNSS) heights to orthometric heights. The geometric method for computing the geoid has been extensively used for a comparatively small region, which, in some points, interpolates geoid heights based on GNSS-derived heights and levelling heights. Several considerations should be considered when using the geometric method to increase the accuracy of a local geoid. Kuwait is used as a test area in this paper to investigate several features of the geometric method. The achievable precision is one of these aspects, the role of the interpolation method, global geopotential models, and the influence of the topographic effect. The accuracy of the local geoid can be substantially enhanced by integrating a geopotential model with a digital terrain model of the research region. It is possible to get a precision of 2–3 cm.

**Keywords:** Geometric Geoid, GNSS/Leveling, Global Geopotential Models, Residual Terrain Model, Kuwait

## 1 Introduction

Geodesy, surveying, geophysics, and a variety of geosciences depend greatly on the geoid because it can be used as a primary datum for determining height differences and gravity potential field [1]. The widespread and rapid use of Global Navigation Satellite Systems (GNSS) has revolutionized surveying, mapping, and navigation, and has replaced time-consuming traditional techniques. GNSS, in particular, can produce geodetic measurements with high accuracy in a fraction of the time. The ellip-

soidal heights are provided by GNSS, which are three-dimensional systems that offer heights relative to an ellipsoid surface. Regrettably, ellipsoidal height is merely a geometrical quantity, Its conversion to orthometric height using the geoid model is commonly used in practically all day-to-day applications that require height data [2].

As a result, determining a high-resolution geoid has become critical to dealing with the possibility of a high level of height accuracy from GNSS, such that the orthometric height can be achieved by integrating the Geoid and GNSS e. g. [1–3].

Based on the development methodologies and data used, the geoid determination methods are separated into four types: Gravimetric, Astrogeodetic, Hybrid, and Geometric. Gravimetric solutions are based on gravity data [4–8]. The measurement of latitude, longitude and vertical deflection using astronomical instruments can be used to determine the Astrogeodetic geoid [9, 10]. Gravimetric geoid tilts concerning GPS/leveling data are used to create the Hybrid [2, 11, 12]. The Geometric method makes use of observed values of Orthometric height and ellipsoidal height to define the geoidal height. These are then went to predict (N) by interpolation at stations at which the only (h) is known. This method is proscribed by the number and distribution of points with known ellipsoidal and orthometric height to suitable levels of accuracy. A further limitation is imposed by the interpolation algorithm chosen for the estimation. For example, linear interpolation assumes that the undulation (N) is linear between the data points [13–17].

The performance of the geometric method is difficult to check for reliability with errors corrupting the output directly. The benefits are that it is conceptually simple and easy to implement with adequate data. To increase the precision of a local geoid created using the geometric method, a well-known Global Geopotential Model (GGM) and local terrain information by Residual Terrain Model (RTM) should be incorporated [13, 15, 18, 19].

The study aims to evaluate numerous interpolation methods i. e., Inverse distance to a power [16, 20], local polynomial [21–24], Kriging [25, 26], Minimum curvature [27–32], Nearest neighbor [33–35], Polynomial Regression [27, 31, 32, 36, 37], Radial basis function [31, 32, 38–40], Modified Shepard's [41, 42], Triangulation with Linear interpolation [31, 32, 43–45], Natural neighbor [31, 32, 46–

**\*Corresponding author: Ahmed Zaki**, Civil Engineering Department, Faculty of Engineering, Delta University for Science and Technology, Gamasa, Egypt, e-mail: [eng\\_zaki\\_2222@ahoo.com](mailto:eng_zaki_2222@ahoo.com)

**Yasmeen Elberry, Mostafa Rabah, Rasha Abd El Ghany**, Department of Civil Engineering, Benha Faculty of Engineering, Benha University, Benha, Egypt, e-mails: [yasmeenelberry1352@gmail.com](mailto:yasmeenelberry1352@gmail.com), [mrabah@bhit.bu.edu.eg](mailto:mrabah@bhit.bu.edu.eg), [Rasha\\_AbdEl\\_Ghany@yahoo.com](mailto:Rasha_AbdEl_Ghany@yahoo.com)

**Hamad Al-Ajami**, Member of Training Authority, Public Authority for Applied Education and Training, Adailiyah, Safat, Kuwait, e-mail: [Hamad\\_AlAjami@yahoo.com](mailto:Hamad_AlAjami@yahoo.com)

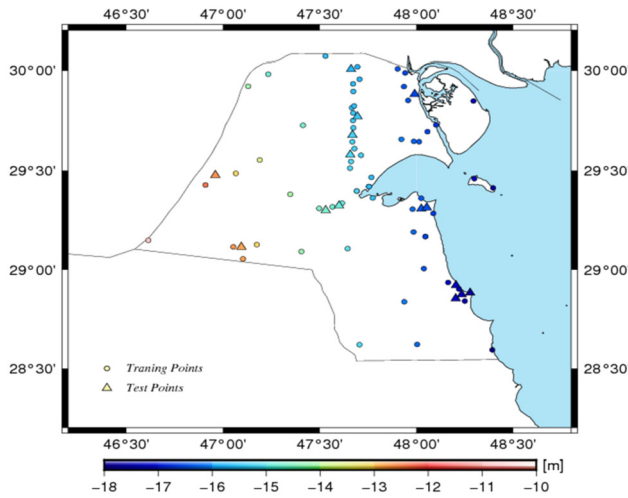
Q1

Q2

52  
53  
54  
55  
56  
57  
58  
59  
60  
61  
62  
63  
64  
65  
66  
67  
68  
69  
70  
71  
72  
73  
74  
75  
76  
77  
78  
79  
80  
81  
82  
83  
84  
85  
86  
87  
88  
89  
90  
91  
92  
93  
94  
95  
96  
97  
98  
99  
100  
101  
102

**Table 1:** Parameters for statistically analysing data sets.

Dataset	Parameter	Mean	STD	CV	Min	Max	SK
Training	$\varphi$	29.409	0.399	0.01	28.585	30.070	-0.257
	$\lambda$	47.731	0.410	0.01	46.613	48.396	-0.68
	$N$	-15.540	1.482	-0.09	-18.546	-10.959	0.806
Testing	$\varphi$	29.427	0.355	0.012	28.841	29.989	-0.027
	$\lambda$	47.598	0.460	0.009	46.796	48.249	-0.515
	$N$	-15.090	1.624	-0.108	-17.396	-12.596	0.462

**Figure 1:** Kuwait's 83 GPS/Levelling stations are distributed across the country.

50], and Moving average [51, 52] in the interpolation of the geometric geoid for the Kuwait state.

## 2 Data

### 2.1 GPS/levelling points

In this study, 83 GPS/Leveling stations were employed. The spread of the network is presented in Figure 1. Since 2016, the GPS/levelling data were collected and made available for this study by Vision International Co., Kuwait. The ITRF2008 datum was used to produce the benchmark GPS coordinates using the Static and Rapid-Static measurement methods using a dual-frequency GPS receiver. The approximate accuracy of GPS coordinates is  $\pm 1.0$  and  $\pm 1.5$  cm, respectively, in horizontal and vertical directions [53].

Using high precision spirit levelling from the Ministry of Defense's (MoD) benchmarks network, the orthometric heights of the benchmarks were produced in this manner.

The MoD networks have been referred to as vertical data of the Kuwait Public Works Department (Kuwait PWD). The Kuwait Oil Company defines PWD as the Mean-Low-Water in Kuwait City (about 1.03 m below mean sea level) [54]. The orthometric heights' absolute accuracy is about  $\pm 1.0$  cm. The geoid undulation based on GPS /Levelling ranges from  $-18.546$  to  $-10.959$  m with a mean value of  $-15.453$  m and a standard deviation of 1.51 m [53].

The statistical interpretation of the data used is summarized in Table 1. The available GPS/levelling data are for 83 stations which were divided into 66 training points used in interpolation for all methods, and 17 testing points to check the accuracy of each method and to know the best method of them as presented in Figure 1. From Table 1, it can be seen that the distributions of input variables in the training and testing stages are approximately the same. In this research we looked into, The geoid undulation ( $N$ ) calculated from station geodetic latitudes ( $\varphi$ ) and longitudes ( $\lambda$ ). The Mean, The standard deviation of variables is abbreviated as STD, The coefficient of variations as STD/Mean is referred to as CV, The skewness of data is denoted by SK, and Min and Max are the minimum and maximum data points, respectively. The skewness of the data is modest, as seen in Table 1, with the geoid undulation having the most skewed distribution in both data sets, followed by longitude and latitude. This indicates that Kuwait has a higher degree of geoid undulation distortion from the normal distribution than the longitude and latitude. For data sets that will be used for both training and testing, the CV is nearly identical.

### 2.2 Digital elevation model (DEM)

Kuwait has a flat topography, with a slightly uneven desert. On the Arabian Gulf's eastern coast, the earth's descended grades steadily from sea level to the west and southwest. The southwestern angle rises 300 meters above sea level. Small hills can be seen all over Kuwait, including along the

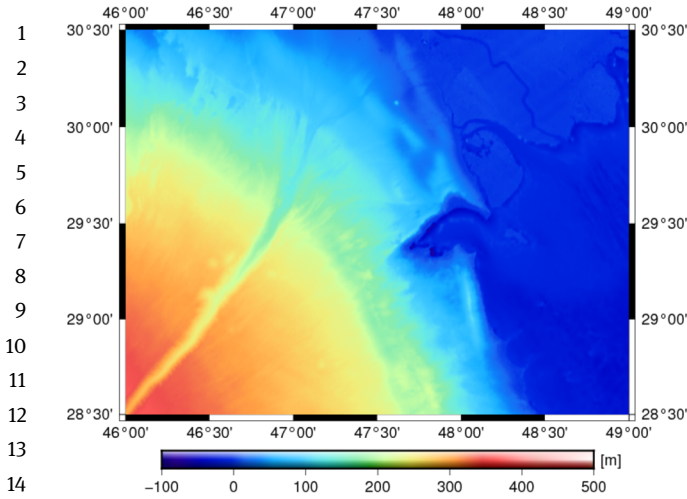


Figure 2: Kuwait's combined DEM with a resolution of  $3'' \times 3''$  [53].

Jal Al-Zour ridge, which has a view of Kuwait Bay's northern coast. This ridge rises to 145 meters in height.

For this study, the DEM for Kuwait was constructed by combining the 3-arcsecond spatial resolution of the Shuttle Radar Topography Mission (SRTM) [55] for land with the 15-arcsecond resolution of the SRTM+ 15 [56] bathymetry depths (see Figure 2) [53]. The model used covers the window from  $27.4^\circ$  N to  $31.2^\circ$  N,  $45.4^\circ$  E to  $49.4^\circ$  E.

### 2.3 Global geopotential model

The Global Geopotential Model (GGM) is a mathematical model that approximates the Earth's external gravitational potential. Combined and Satellite-only are the two categories of GGMs available. Without any direct contribution from terrestrial data, the former is calculated using satellite-only measures like GOCE [57], GRACE [58], and CHAMP [59, 60]. [53] GGMs have been investigated in Kuwait. According to their research, the EIGEN-6C4 and XGM2016 models at their highest degree, as well as the most suited Spherical Harmonics (SH) degree-and-order (d/o) for Kuwait, are the best combined GGMs models for application in Kuwait GOCE GGMs are 250 according to the Space Wise model (SPW\_R5) [61] with EGM2008 [62] up to SH d/o 2190. (SPW R5) is included in this study. As synthesized, the coefficient model as recovered from the study of the GOCE grids generates grids that are very similar to the original ones, but it is somewhat different due to a global regularization (based on Monte Carlo samples): stronger globally, but it is inevitably smoothing a very small portion of the signal at the very high frequencies.

## 3 Method

As is well known,  $h_{\text{Ellipsoid}}$  and  $H_{\text{Orthometric}}$  signify the ellipsoidal heights from GPS observation and the orthometric heights at some points, respectively. Equation 1 [10] shows how to calculate the geoid heights at these points.

$$N_{\text{GPS/Levelling}} = h_{\text{Ellipsoid}} - H_{\text{Orthometric}} \quad (1)$$

Values  $N_{\text{GPS/Levelling}}$  values obtained in this way are referred to as observed geoid heights. An interpolation method can be used to forecast the geoid heights at any other point. This is the most common method for creating a local geoid in a confined area. After determining the geoid heights at other points of interest, the GPS-derived heights at these points can be transformed into orthometric heights. The following method is advised to enhance the precision of the established geoid. As it is obvious, the height of a geoid can be split into three components i. e.  $N_{\text{GGM}}$ ,  $N_r$ , and  $N_{\text{RTM}}$  as [63, 64]:

$$N_{\text{GPS/Levelling}} = N_{\text{GGM}} + N_r + N_{\text{RTM}} \quad (2)$$

$N_{\text{GGM}}$  denotes the long-wavelength constituent, this can be calculated with the use of a geopotential model; The medium or residual wavelength component is called  $N_r$ , and it may be calculated using the Stokes integral of a gravity anomaly in the ground, and  $N_{\text{RTM}}$  is terrain effect.

Because gravity measurements are not always accessible in a given location, Equation 2 could be written as:

$$N_r = N_{\text{GPS/Levelling}} - N_{\text{GGM}} - N_{\text{RTM}} \quad (3)$$

where  $N_{\text{GPS/Levelling}}$  is the observed geoid height, and  $N_{\text{GGM}}$  and  $N_{\text{RTM}}$  are calculated, respectively, from a geopotential model and a digital terrain model. Equation 3 gives the component values at observation points. The matching values at any other points of interest are interpolated from these values  $N_r$ . The values  $N$  forecasting points are determined using Equation 2 once the predicted values  $\hat{N}_r$  are acquired.

$$N = \hat{N}_{\text{GGM}} + \hat{N}_r + \hat{N}_{\text{RTM}} \quad (4)$$

Components with a long wavelength and terrain corrections at the predicted points are denoted by  $\hat{N}_{\text{GGM}}$  and  $\hat{N}_r$ .  $\hat{N}_{\text{GGM}}$  can be expressed as follows [3]:

$$\begin{aligned} N_{\text{GGM}} &= \frac{GM}{\gamma r} \sum_{n=2}^{\infty} \\ &= \left(\frac{a}{r}\right)^n \sum_{m=0}^n (\bar{C}_{nm} \cos m\lambda + \bar{S}_{nm} \sin m\lambda) \bar{P}_{nm}(\cos \theta) \end{aligned} \quad (5)$$

52  
53  
54  
55  
56  
57  
58  
59  
60 Q3  
61  
62  
63  
64  
65  
66  
67  
68  
69  
70  
71  
72  
73  
74  
75  
76  
77  
78  
79  
80  
81  
82  
83  
84  
85  
86  
87  
88  
89  
90  
91  
92  
93  
94  
95  
96  
97  
98  
99  
100  
101  
102

Where  $GM$  stands for the geocentric gravitational constant.; The geocentric radius is  $r$ ; The ellipsoid's semi-major axis is denoted by  $a$ ;  $\bar{C}_{nm}$ ,  $\bar{S}_{nm}$  and  $\bar{P}_{nm}$  are the completely normalized cosine, sine, and associate coefficients, respectively;  $\lambda$  is the geodetic longitude;  $\theta$  represents the polar distance, and  $\gamma$  is the normal gravity.

The  $N_{RTM}$  is the effect due to the topographic reduction which can be computed as presented in Equation 4 [65]:

$$N_{RTM} = \frac{G}{\gamma} \iint_E \int_{H_{ref}}^{h'} \frac{\rho(x, y, z)}{[(x_P - x)^2 + (y_P - y)^2 + (h_P - z)^2]^{\frac{1}{2}}} dx dy dz \quad (6)$$

where  $G$  signifies the gravitational constant of Newton,  $\gamma$  is the normal gravity, the integration area's planar projection is denoted by  $E$ , the smoothed DEM's height is represented by  $H_{ref}$ , the height of the detailed DEM is  $h'$ , the integrated topography's Cartesian coordinates are  $x$ ,  $y$ , and  $z$ , the mean reference is  $\rho(x, y, z)$ ,  $2.67 \text{ g.cm}^{-3}$  is the density of the Earth's crust, in the Cartesian coordinates system,  $x_P$ ,  $y_P$ , and  $h_P$  denote the coordinates and height of the computational point.

Interpolation is a critical stage in the geoid determination process in mathematics, there are a variety of interpolation methods. In this study 11 interpolation methods by using Golden Software Surfer V.23.2.176: Inverse distance to power, Radial basis function, Local polynomial, Nearest neighbor, Minimum curvature, Polynomial Regression (Cubic), Modified Shepard's, Triangulation with Linear interpolation, Kriging Natural neighbor, and Moving average are used for comparison.

## 4 Results and discussion

According to Equation 3,  $N_r$  is computed at the 66 training stations by removing the components of  $N_{GGM}$  and  $N_{RTM}$ . Removing the effects of the long wavelengths ( $N_{GGM}$ ) has been fulfilled by removing the effect of the composite reference GGM from Space-Wise-Model (SPW\_R5) up to degree-and-order (d/o) 250 with EGM2008 from (d/o) 251 to SH d/o 2190 was used by using Gravsoft software [66]. The topographic effect ( $N_{RTM}$ ) is computed by the RTM model [65] and TC-program [66] for all masses within a radius of 100 km about the computational point.

The aforementioned 11 interpolation method is used to compute the geometric geoid model over the Kuwait state with a grid of  $5 \text{ km} \times 5 \text{ km}$ . Figure 3 to Figure 13 shows the computed geoid models from each interpolation method.

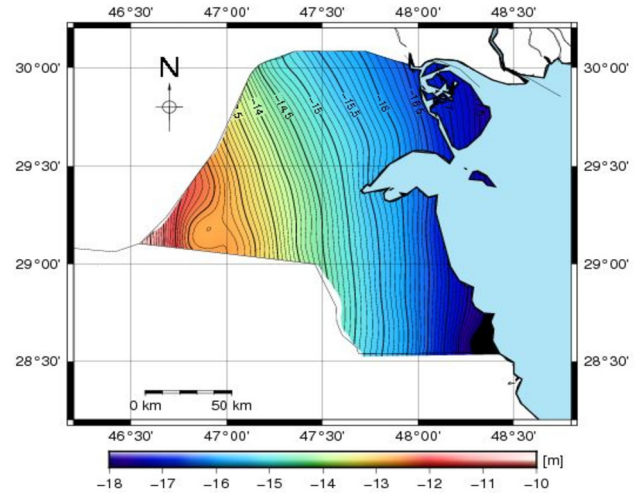


Figure 3: The geometric geoid model by Inverse distance to a power method.

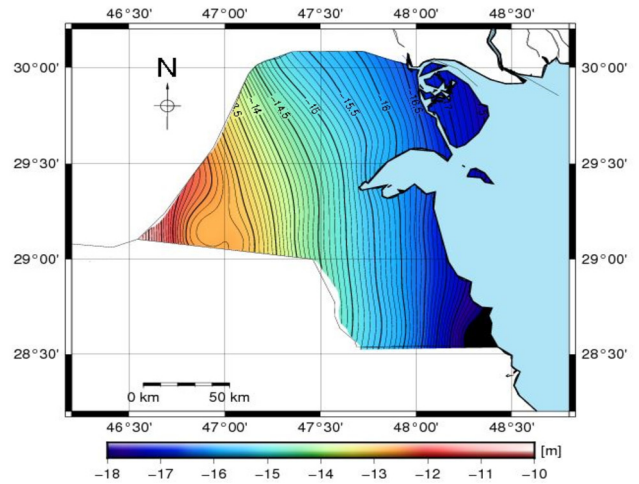


Figure 4: The geometric geoid model by the Kriging method.

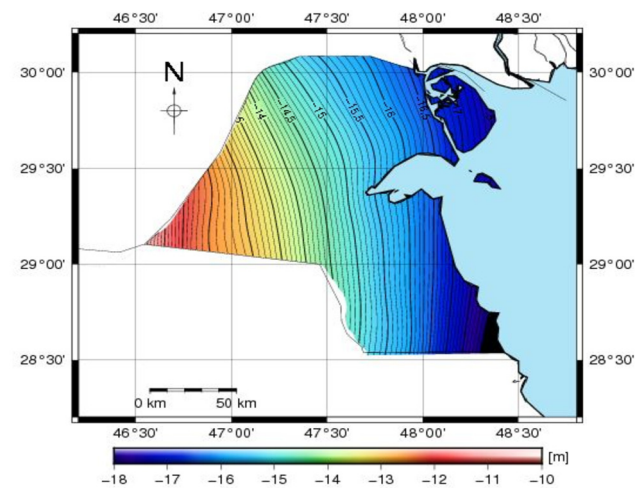


Figure 5: The geometric geoid model by Local polynomial method.

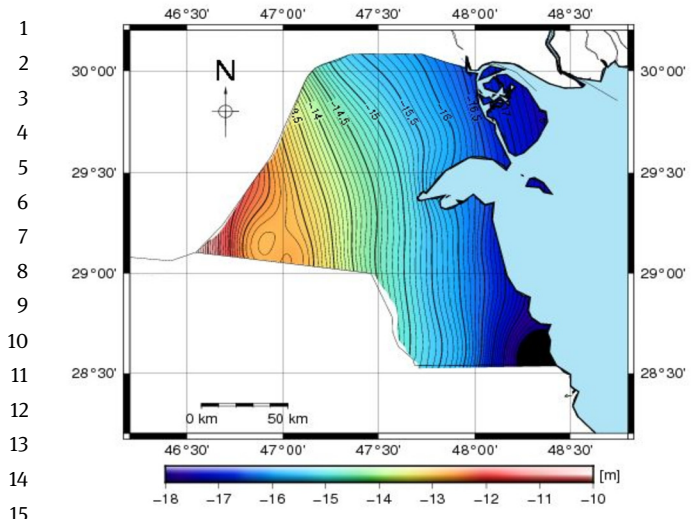


Figure 6: The geometric geoid model by Minimum curvature method.

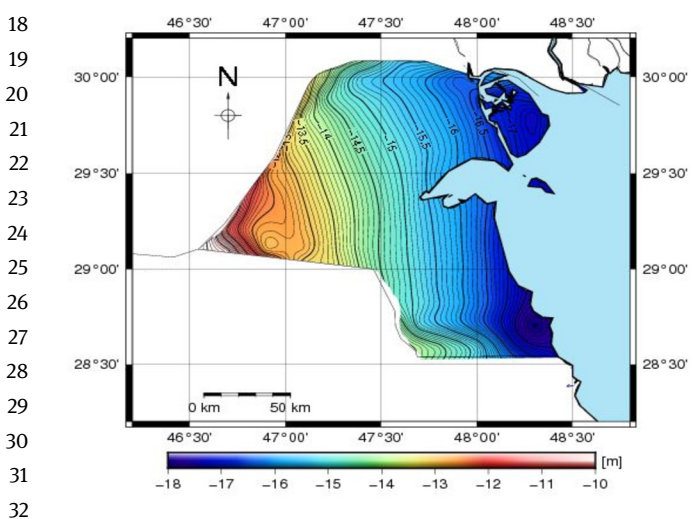


Figure 7: The geometric geoid model by the Triangulation method.

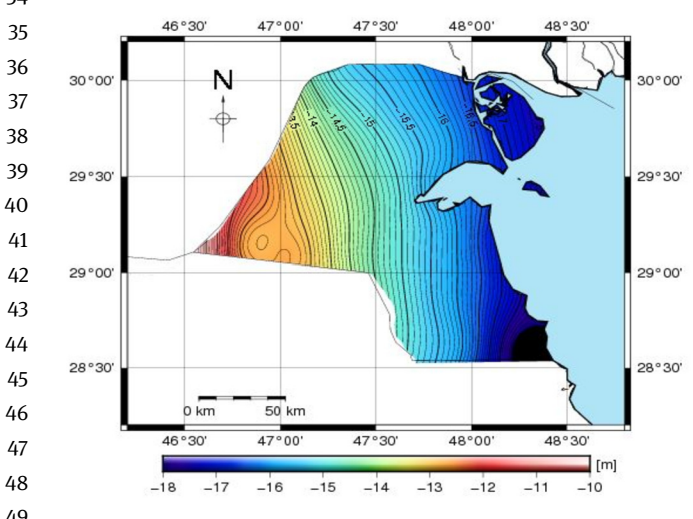


Figure 8: The geometric geoid model by Radial basis function method.

51

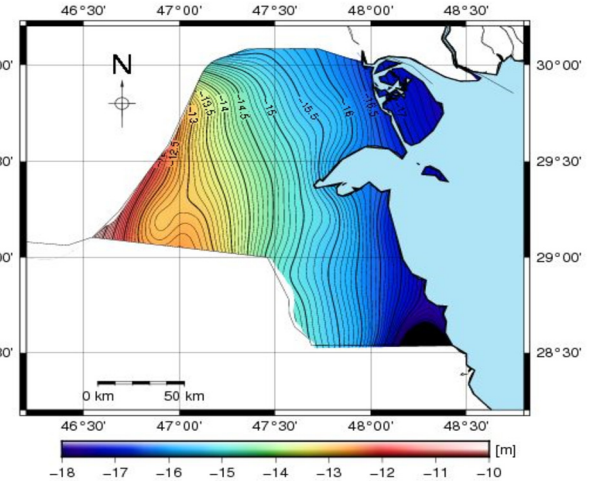


Figure 9: The geometric geoid model by Modified Shepard method.

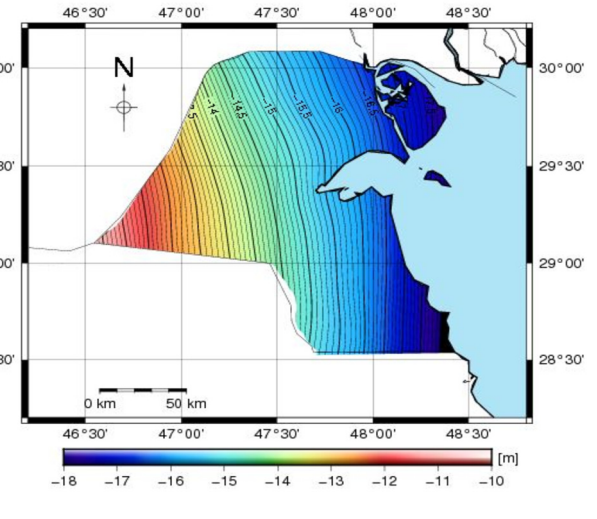


Figure 10: The geometric geoid model by the Moving average method.

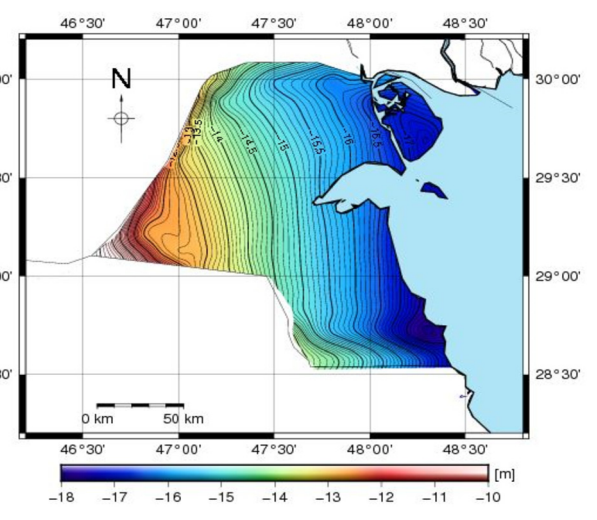


Figure 11: The geometric geoid model by Natural neighbor method.

52  
53  
54  
55  
56  
57  
58  
59  
60  
61  
62  
63  
64  
65  
66  
67  
68  
69  
70  
71  
72  
73  
74  
75  
76  
77  
78  
79  
80  
81  
82  
83  
84  
85  
86  
87  
88  
89  
90  
91  
92  
93  
94  
95  
96  
97  
98  
99  
100  
101  
102

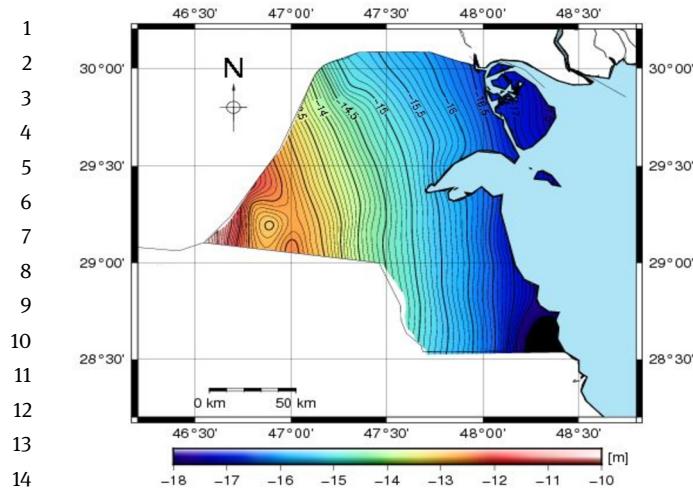


Figure 12: The geometric geoid model by the Nearest neighbor method.

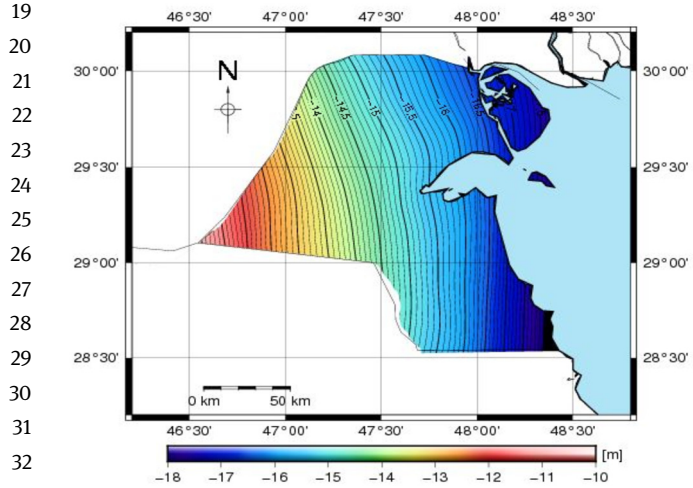


Figure 13: The geometric geoid model by the Polynomial regression method.

To evaluation of the interpolation methods, after then, the geoid heights at each of the 17 test points were anticipated and compared to known values. The results are shown in Table 2. The STD varies from 0.0211 m to 0.272 m. This implies that the choice of the interpolation method is very significant in the determination of the geometric geoid. Among them, the Modified Shepard’s method has the smallest STD with 0.0211 m. Taking into account the observed geoid heights at these test points with an accuracy of roughly 1 cm, the accuracy of Minimum curvature, Radial basis function Nearest neighbor, and Kriging one be the same. The worse results have been acquired from the Triangulation with linear interpolation, Polynomial Regression (Cubic), Natural neighbor, and Moving av-

Table 2: Comparison between the computed geoid models and 17 test points.

Interpolation method	Min	Max	Mean	STD
Inverse distance to a power	-0.0939	0.061	-0.0028	0.0429
Natural neighbor	-0.727	0.099	-0.055	0.1912
Kriging	-0.0483	0.06014	-0.0037	0.0289
Local polynomial	-0.3801	0.192	-0.0033	0.153
Minimum curvature	-0.0478	0.029	-0.0026	0.0231
Modified shepard’s method	-0.0416	0.0213	-0.00421	0.0211
Moving average	-0.7422	0.2142	-0.0386	0.272
Nearest neighbor	-0.0563	0.0323	-0.00245	0.0228
Polynomial Regression (Cubic)	-0.627	0.3047	-0.0203	0.2444
Radial basis function	-0.0477	0.0606	-0.000626	0.0256
Triangulation with linear interpolation	-0.6115	0.1189	-0.0436	0.1626

erage with STD varies from 0.1626 m to 0.272 m. The worse result has been obtained from the Moving average method with STD 0.272 m.

### 5 Conclusions

According to this study, the geometric method can produce a precise local geoid for Kuwait with a precision of 2–3 cm. This is analogous to geoid heights generated by GPS/leveling. The accuracy of Inverse Distance to a power, Nearest neighbor, local polynomial, Kriging, Minimum curvature, Polynomial Regression (Cubic), Modified Shepard’s, Natural neighbor, Radial basis function, Triangulation with Linear, and Moving average models in this study, use of GPS/leveling data inputs in modelling geoid undulation in Kuwait was examined. The errors of these models were compared using the variations in Mean and standard deviation (STD) values. Modified Shepard’s model performed better in the geometric geoid determination for Kuwait, according to the models used in this study.

**Declaration of interests:** The authors declare that they have no known competing financial interests or personal relationships that could have appeared to influence the work reported in this paper.

### References

[1] B. Hofmann-Wellenhof and H. Moritz, *Physical Geodesy*. Springer Science and Business Media, 2006.

52  
53  
54  
55  
56  
57  
58  
59  
60  
61  
62  
63  
64  
65  
66  
67  
68  
69  
70  
71  
72  
73  
74  
75  
76 Q5  
77  
78  
79  
80  
81  
82  
83  
84  
85  
86  
87  
88  
89  
90  
91  
92  
93  
94  
95  
96  
97  
98  
99  
100  
101  
102

- [2] W. Torge and J. Müller, *Geodesy*. Walter de Gruyter, 2012.
- [3] F. Sansò and M. G. Sideris, *Geoid determination: theory and methods*. Springer Science and Business Media, 2013.
- [4] A. Zaki and S. Mogren, "A high-resolution gravimetric geoid model for Kingdom of Saudi Arabia," *Surv. Rev.*, pp. 1–16, 2021, doi: 10.1080/00396265.2021.1944544.
- [5] H. Al-Ajami, A. Zaki, M. Rabah, and M. El-Ashquer, "A High-Resolution Gravimetric Geoid Model for Kuwait Using the Least-Squares Collocation," *Front. Earth Sci.*, vol. 9, 2022, doi: 10.3389/feart.2021.753269.
- [6] Y. M. Wang, J. Saleh, X. Li, and D. R. Roman, "The US Gravimetric Geoid of 2009 (USGG2009): model development and evaluation," *J. Geod.*, vol. 86, no. 3, pp. 165–180, 2012, doi: 10.1007/s00190-011-0506-7.
- [7] J. Huang and M. Véronneau, "Canadian gravimetric geoid model 2010," *J. Geod.*, vol. 87, no. 8, pp. 771–790, 2013, doi: 10.1007/s00190-013-0645-0.
- [8] A. Saadon, M. El-Ashquer, B. Elsaka, and G. El-Fiky, "Determination of local gravimetric geoid model over Egypt using LSC and FFT estimation techniques based on different satellite-and ground-based datasets," *Surv. Rev.*, pp. 1–11, 2021.
- [9] W. A. Heiskanen and H. Moritz, "Physical geodesy (Book on physical geodesy covering potential theory, gravity fields, gravimetric and astrogeodetic methods, statistical analysis, etc)," 1967.
- [10] W. Heiskanen and H. Moritz, "Physical Geodesy WH Freeman and Company San Francisco," *London Google Sch.*, 1967.
- [11] A. Zaki, "Assessment of GOCE models in Egypt," Master Thesis, Faculty of engineering, Cairo university, Egypt, 2015.
- [12] M. El-Ashquer, B. Elsaka, and G. El-Fiky, "EGY-HGM2016: an improved hybrid local geoid model for Egypt based on the combination of GOCE-based geopotential model with gravimetric and GNSS/levelling measurements," *Arab. J. Geosci.*, vol. 10, no. 11, p. 251, 2017, doi: 10.1007/s12517-017-3042-9.
- [13] M. R. Kaloop, S. Pijush, M. Rabah, H. Al-Ajami, J. W. Hu, and A. Zaki, "Improving accuracy of local geoid model using machine learning approaches and residuals of GPS/levelling geoid height," *Surv. Rev.*, pp. 1–14, Aug. 2021, doi: 10.1080/00396265.2021.1970918.
- [14] M. R. Kaloop, M. Rabah, J. W. Hu, and A. Zaki, "Using advanced soft computing techniques for regional shoreline geoid model estimation and evaluation," *Mar. Georesources Geotechnol.*, vol. 36, no. 6, pp. 688–697, 2018.
- [15] M. R. Kaloop, A. Zaki, H. Al-Ajami, and M. Rabah, "Optimizing local geoid Undulation model using GPS/levelling measurements and heuristic regression approaches," *Surv. Rev.*, vol. 52, no. 375, pp. 544–554, 2020.
- [16] B. Erol and R. N. Çelik, "Modelling Local Gps/Levelling Geoid With the Assessment of Inverse Distance Weighting and Geostatistical Kriging Methods," *Civ. Eng.*, 2000.
- [17] H.-J. Götze, "Gravity Method, Principles," in *Encyclopedia of Solid Earth Geophysics*, H. K. Gupta, Ed. Dordrecht: Springer Netherlands, 2011, pp. 500–504. doi: 10.1007/978-90-481-8702-7\_93.
- [18] K. P. Schwarz, "Data types and their spectral properties," *Local gravity F. Approx. Beijing Int. Geoid Determ. Summer Sch.*, 1984.
- [19] Y. Zhan-ji and C. Yong-qi, "Determination of local geoid with geometric method: Case study," *J. Surv. Eng.*, vol. 125, no. 3, pp. 136–146, 1999.
- [20] D. E. Watson, "Contouring: A Guide to the Analysis and Display of Spatial Data, Tarrytown, NY." Pergamon (Elsevier Science, Inc.), 1992.
- [21] D. Kidner, M. Dorey, and D. Smith, "What's the point? Interpolation and extrapolation with a regular grid DEM," 1999.
- [22] W. Harlan, "Avoiding interpolation artifacts in Stolt migration," *SEP-30 Stanford Explor. Proj.*, vol. 30, pp. 103–110, 1982.
- [23] M. Yanalak and O. Baykal, "Digital elevation model based volume calculations using topographical data," *J. Surv. Eng.*, vol. 129, no. 2, pp. 56–64, 2003.
- [24] G. Petrie and T. J. M. Kennie, "Terrain modelling in surveying and civil engineering," *Comput. Des.*, vol. 19, no. 4, pp. 171–187, 1987.
- [25] N. Cressie, C. A. Gotway, and M. O. Grondona, "Spatial prediction from networks," *Chemom. Intell. Lab. Syst.*, vol. 7, no. 3, pp. 251–271, 1990.
- [26] S. Golden, "Surfer 8 contouring and 3D surface mapping for scientists and engineers user's guide. Golden Software," *Inc., Color. USA*, www.goldensoftware.com, 2002.
- [27] I. C. Briggs, "Machine contouring using minimum curvature," *Geophysics*, vol. 39, no. 1, pp. 39–48, 1974.
- [28] W. H. F. Smith and P. Wessel, "Gridding with continuous curvature splines in tension," *Geophysics*, vol. 55, no. 3, pp. 293–305, 1990.
- [29] C. U. I. Fangpeng, H. U. Ruilin, L. I. U. Zhaolian, and Y. U. Wenlong, "Surfer Software Platform Based Complex Three-Dimensional Geological Digital Models for Pre-Processing of FLAC<sup>3D</sup>," *工程地质学报*, vol. 16, no. 5, pp. 699–702, 2008.
- [30] C. P. Oden and C. Moulton, *GP workbench manual: Technical manual, user's guide, and software guide*. US Geological Survey, 2006.
- [31] I. Golden Software, "Surfer User's Guide," *Golden Software, Inc.*, p. 665, 2002.
- [32] G. Software, "Full User's Guide," 2015.
- [33] B. D. Ripley, *Statistical inference for spatial processes*. Cambridge university press, 1991.
- [34] R. Webster and M. A. Oliver, *Geostatistics for environmental scientists*. John Wiley & Sons, 2007.
- [35] P. Burrough and R. McDonnell, "Spatial information systems and geostatistics," *Princ. Geogr. Inf. Syst.*, vol. 333, 1998.
- [36] L. Brutman, "Lebesgue functions for polynomial interpolation-a survey," *Ann. Numer. Math.*, vol. 4, pp. 111–128, 1996.
- [37] E. Süli and D. F. Mayers, *An introduction to numerical analysis*. Cambridge university press, 2003.
- [38] R. L. Hardy, "Theory and applications of the multiquadric-biharmonic method 20 years of discovery 1968–1988," *Comput. Math. with Appl.*, vol. 19, no. 8–9, pp. 163–208, 1990.
- [39] M. J. D. Powell, "The theory of radial basis function approximation in 1990," *Adv. Numer. Anal.*, pp. 105–210, 1992.
- [40] R. E. Carlson and T. A. Foley, "The parameter R2 in multiquadric interpolation," *Comput. Math. with Appl.*, vol. 21, no. 9, pp. 29–42, 1991.
- [41] R. J. Renka, "Multivariate interpolation of large sets of scattered data," *ACM Trans. Math. Softw.*, vol. 14, no. 2,

- 1 pp. 139–148, 1988.
- 2 [42] R. Franke and G. Nielson, “Smooth interpolation of large sets  
3 of scattered data,” *Int. J. Numer. Methods Eng.*, vol. 15, no. 11,  
4 pp. 1691–1704, 1980.
- 5 [43] C. L. Lawson, “Software for C1 surface interpolation,”  
6 *Mathematical software*, Elsevier, 1977, pp. 161–194.
- 7 [44] D.-T. Lee and B. J. Schachter, “Two algorithms for constructing  
8 a Delaunay triangulation,” *Int. J. Comput. Inf. Sci.*, vol. 9, no. 3,  
9 pp. 219–242, 1980.
- 10 [45] L. Guibas and J. Stolfi, “Primitives for the manipulation of  
11 general subdivisions and the computation of Voronoi,” *ACM  
12 Trans. Graph.*, vol. 4, no. 2, pp. 74–123, 1985.
- 13 [46] R. Sibson, “A brief description of natural neighbour  
14 interpolation,” *Interpret. Multivar. data*, 1981.
- 15 [47] S. J. Owen, “An implementation of natural neighbor  
16 interpolation in three dimensions.” Brigham Young University,  
17 Department of Engineering, 1992.
- 18 [48] D. Watson, *nnggridr: An implementation of natural neighbor  
19 interpolation*. D. Watson, 1994.
- 20 [49] N. Sukumar, B. Moran, A. Yu. Semenov, and V. V. Belikov,  
21 “Natural neighbour Galerkin methods,” *Int. J. Numer. Methods  
22 Eng.*, vol. 50, no. 1, pp. 1–27, 2001.
- 23 [50] M. Yanalak, “Effect of gridding method on digital terrain model  
24 profile data based on scattered data,” *J. Comput. Civ. Eng.*,  
25 vol. 17, no. 1, pp. 58–67, 2003.
- 26 [51] G.-F. Gu and W.-X. Zhou, “Detrending moving average  
27 algorithm for multifractals,” *Phys. Rev. E*, vol. 82, no. 1,  
28 p. 11136, 2010.
- 29 [52] P. Lanos, M. Le Goff, M. Kovacheva, and E. Schnepf,  
30 “Hierarchical modelling of archaeomagnetic data and curve  
31 estimation by moving average technique,” *Geophys. J. Int.*,  
32 vol. 160, no. 2, pp. 440–476, 2005.
- 33 [53] M. El-Ashquer, H. Al-Ajami, A. Zaki, and M. Rabah, “Study  
34 on the selection of optimal global geopotential models for  
35 geoid determination in Kuwait,” *Surv. Rev.*, vol. 52, no. 373,  
36 pp. 373–382, 2020.
- 37 [54] M. Rabah, “Using RTK tides on the northern coast of Egypt:  
38 Undulation model corrections from EGM2008,” *Civ. Eng. Surv.  
39 Sept.*, pp. 43–47, 2009.
- 40 [55] M. Werner, “Shuttle radar topography mission (SRTM) mission  
41 overview,” *Frequenz*, vol. 55, no. 3–4, pp. 75–79, 2001.
- 42 [56] C. J. Olson, J. J. Becker, and D. T. Sandwell, “A new global  
43 bathymetry map at 15 arcsecond resolution for resolving  
44 seafloor fabric: SRTM15\_PLUS,” *AGU Fall Meeting Abstracts*,  
45 2014, vol. 2014, OS34A-03.
- 46 [57] M. R. Drinkwater, R. Floberghagen, R. Haagmans, D. Muzi,  
47 and A. Popescu, “VII: Closing session: GOCE: ESA’s first  
48 earth explorer core mission,” *Space Sci. Rev.*, vol. 108, no. 1,  
49 pp. 419–432, 2003.
- 50 [58] P. J. Yeh, S. C. Swenson, J. S. Famiglietti, and M. Rodell,  
51 “Remote sensing of groundwater storage changes in Illinois  
52 using the Gravity Recovery and Climate Experiment (GRACE),”  
53 *Water Resour. Res.*, vol. 42, no. 12, 2006.
- 54 [59] C. Reigber, P. Schwintzer, and H. Lühr, “The CHAMP  
55 geopotential mission,” *Boll. Geof. Teor. Appl.*, vol. 40,  
56 pp. 285–289, 1999.
- 57 [60] S. M. Hoover, L. S. Clark, D. F. Alters, L. Hood, and J. G. Champ,  
58 *Media, home, and family*. Psychology Press, 2004.
- 59 [61] A. Gatti, M. Reguzzoni, F. Migliaccio, and F. Sansò,  
60 “Computation and assessment of the fifth release of the  
61 GOCE-only space-wise solution,” *The 1st joint commission 2  
62 and IGFS meeting*, 2016, pp. 19–23.
- 63 [62] N. K. Pavlis, S. A. Holmes, S. C. Kenyon, and J. K. Factor, “The  
64 EGM2008 global gravitational model,” *AGU Fall Meeting  
65 Abstracts*, 2008, vol. 2008, G22A-01.
- 66 [63] N. Srinivas *et al.*, “Gravimetric geoid of a part of south  
67 India and its comparison with global geopotential models  
68 and GPS-levelling data,” *J. earth Syst. Sci.*, vol. 121, no. 4,  
69 pp. 1025–1032, 2012.
- 70 [64] C. Tocho and G. S. Vergos, “Assessment of different-generation  
71 GOCE-only and GOCE/GRACE Earth Global Gravity Models  
72 over Argentina using terrestrial gravity anomalies and  
73 GPS/Levelling data,” *Newton’s Bull.*, vol. 5, pp. 105–126, 2015.
- 74 [65] R. Forsberg, A study of terrain reductions, density anomalies  
75 and geophysical inversion methods in gravity field modelling,  
76 Ohio State University. Dept of Geodetic Science and Surveying.  
77 Report No. OSU/DGSS-355, 1984.
- 78 [66] R. Forsberg and C. C. Tscherning, “GRAVSOFIT,” *Geod. gravity F.  
79 Model. programs (overview manual)*, 2008.
- 80  
81  
82  
83  
84  
85  
86  
87  
88  
89  
90  
91  
92  
93  
94  
95  
96  
97  
98  
99  
100  
101  
102